International Journal of Chemical, Materials and Biomolecular Sciences
ISSN: 2415-6620
Vol:10, No:6, 2016

Tensile and Fracture Properties of Cast and Forged Composite Synthesized by Addition of *in-situ* Generated Al_3Ti-Al_2O_3 Particles to Magnesium

H. M. Nanjundaswamy, S. K. Nath, S. Ray

Abstract**—**TiO_2 particles have been added in molten aluminium to result in aluminium based cast Al/Al_3Ti-Al_2O_3 composite, which has been added then to molten magnesium to synthesize magnesium based cast Mg-Al/Al_3Ti-Al_2O_3 composite. The nominal compositions in terms of Mg, Al, and TiO_2 contents in the magnesium based composites are Mg-9Al-0.6TiO_2, Mg-9Al-0.8TiO_2, Mg-9Al-1.0TiO_2 and Mg-9Al-1.2TiO_2 designated respectively as MA6T, MA8T, MA10T and MA12T. The microstructure of the cast magnesium based composite shows grayish rods of intermetallics Al_3Ti, inherited from aluminium based composite but these rods, on hot forging, breaks into smaller lengths decreasing the average aspect ratio (length to diameter) from 7.5 to 3.0. There are also cavities in between the broken segments of rods. β-phase in cast microstructure, $Mg_{17}Al_{12}$, dissolves during heating prior to forging and re-precipitates as relatively finer particles on cooling. The amount of β-phase also decreases on forging as segregation is removed. In both the cast and forged composite, the Brinell hardness increases rapidly with increasing addition of TiO_2 but the hardness is higher in forged composites by about 80 BHN. With addition of higher level of TiO_2 in magnesium based cast composite, yield strength decreases progressively but there is marginal increase in yield strength over that of the cast Mg-9 wt. pct. Al, designated as MA alloy. But the ultimate tensile strength (UTS) in the cast composites decreases with the increasing particle content indicating possibly an early initiation of crack in the brittle inter-dendritic region and their easy propagation through the interfaces of the particles. In forged composites, there is a significant improvement in both yield strength and UTS with increasing TiO_2 addition and also, over those observed in their cast counterpart, but at higher addition it decreases. It may also be noted that as in forged MA alloy, incomplete recovery of forging strain increases the strength of the matrix in the composites and the ductility decreases both in the forged alloy and the composites. Initiation fracture toughness, J_{IC}, decreases drastically in cast composites compared to that in MA alloy due to the presence of intermetallic Al_3Ti and Al_2O_3 particles in the composite. There is drastic reduction of J_{IC} on forging both in the alloy and the composites, possibly due to incomplete recovery of forging strain in both as well as breaking of Al_3Ti rods and the voids between the broken segments of Al_3Ti rods in composites. The ratio of tearing modulus to elastic modulus in cast composites show higher ratio, which increases with the increasing TiO_2 addition. The ratio decreases comparatively more on forging of cast MA alloy than those in forged composites.

Keywords**—**Composite, fracture toughness, forging, tensile properties.

H. M. Nanjundaswamy, Professor is with the PES College of Engineering, Mandya, India (e- mail: hmnanjunda@gmail.com).
S. K. Nath, Professor is with the IIT Roorkee, Roorkee, India.
S. Ray, Professor is with the IIT Mandi, Mandi, India.

I. Introduction

MAGNESIUM alloys, since lighter than aluminum alloys, have received considerable attention for application in the automobile parts, which are anticipated to increase globally at an average rate of 15% per year [1]. Cast magnesium based composites synthesized by addition of cast aluminum based composites resulting Mg-Al/Al_3Ti-Al_2O_3 composites, processed earlier by dispersion of TiO_2 particles in molten aluminum, have inherited intermetallic, Al_3Ti, and alumina particles from the aluminum based composite. The aluminum from the matrix of aluminum based composite has alloyed with the molten magnesium, and the addition has been controlled to obtain a matrix of Mg-9 wt.% Al alloy in all the composites synthesized for this study. Since solidification processing results in casting defects and segregation, the effect of secondary processing like hot forging on the mechanical properties has also been investigated. The matrix alloy composition has similar aluminum content as in AZ91 alloy, which is the most widely used die casting magnesium alloy, offering good combination of castability, corrosion resistance and mechanical properties [2], [3]. For AZ91 alloy, the strengthening is primarily determined by the volume and morphology of intermetallic $Mg_{17}Al_{12}$ phase and the alloy generally fails by brittle cleavage and quasi-cleavage fracture along (0001) crystal plane. Lu et al. [4] have claimed that micro-cracks tend to initiate in the Mg/$Mg_{17}Al_{12}$ interface and even in the $Mg_{17}Al_{12}$ particles leading to fracture.

Magnesium and its alloys have been strengthened further by reinforcing with the intermetallic compounds like TiB_2 and ceramic like SiC. Wang et al. [5] have observed 41%, 106% and 181% increase in hardness over that of cast magnesium by reinforcing magnesium with 10, 20, and 30 vol.% TiB_2 particles respectively by powder metallurgy. In cast AZ91 alloy reinforced with 2, 5 and 7.5 wt.% fine TiB_2 (~7 μm) particles, Wang et al. [6] have observed that hardness increases with increasing the TiB_2 content. However, no tensile properties of these composites have been reported. In AZ91 alloy reinforced with 9.4 vol.% and 15.1 vol.% SiC_p, the yield strengths observed by Lloyd [7] are 191 and 208 MPa respectively, but the UTS in both composites is surprisingly the same 236 MPa. However, the corresponding elongations decrease to 2 and 1% respectively. Hassan and Gupta [8] measured the tensile properties of magnesium reinforced with the fine elemental titanium particles and reported that the presence of titanium reinforcement led to an improvement of 0.2% YS and ductility, while the UTS was marginally

lowered.

Forming limit of Mg alloy shows an excellent workability at temperatures from 250 to 400 °C but at temperatures lower than 200 ºC it is brittle and at temperatures higher than 400 °C there is heavy oxidation [9]. The forged magnesium alloys are reported to show improved mechanical properties than those in the corresponding cast magnesium alloys [10], [11]. The secondary processing of extrusion improves the yield strength and UTS in extruded AZ91D-15 vol.% SiC_p (size~54 μm) composite to 257 MPa and 289 MPa respectively [12]. But, the yield strength of un-reinforced AZ91D alloy is 215 MPa, and its UTS is 296 MPa.

The initiation fracture toughness in magnesium and its alloys have been measured both in terms of K_{IC} and J_{IC}. The decrease in grain size of the extruded magnesium has been observed to increase K_{IC} [13]. Purazrang et al. [14] have observed that squeeze cast AZ91 alloy has K_{IC} 14.4 MPa $m^{1/2}$ but it marginally improves on T6 heat treatment. When 20% δ-alumina short fibers are incorporated in AZ91 alloy by squeeze casting, K_{IC} decreases in spite of improvement in yield strength and tensile strength. T6 heat treatment decreases it further. Purazrang et al. [15] in a later study have observed that K_{IC} decreases with increasing alumina content. Manoharan and Lewandowski [16] have observed in Al-Zn-Mg-Cu alloy based composites that in under-aged composite J_{IC} decreases linearly with increasing volume fraction of SiC, while in over-aged composite a more rapid decrease in J_{IC} is observed. In sand cast AZ91C subjected to T6 heat treatment, Barbagallo et al. [17] has measured both K_{IC} and J_{IC} and observed respectively 21.7 MPa.$m^{1/2}$ and 8.3 X 10^{-3} MPa.m, which are higher than those observed by others. The present work also involves the study of fracture toughness in cast Mg-9 wt.% Al based composite containing intermetallic Al_3Ti and extracted oxide particles and its change on forging).

II. Experimental Procedures

Cast Mg-Al/Al_3Ti-Al_2O_3 composite has been synthesized by adding to molten magnesium cast Al/Al_3Ti-Al_2O_3 composite made earlier by addition of TiO_2 particles in molten aluminum by stir casting technique under inert argon atmosphere. The commercial aluminum and magnesium of chemical composition given in Table I, was used for this study. The melt containing intermetallic Al_3Ti and ceramic Al_2O_3 was cast in the permanent steel mold and cooled by immersing in a water bath. Cast Al/Al_3Ti-Al_2O_3 composite with different TiO_2 content has been used to vary intermetallic Al_3Ti and ceramic Al_2O_3 content in the cast composite while keeping the aluminum content of the matrix to correspond to AZ91 (8.5-9.5 wt.% Al) alloy. The composites were synthesized with nominal compositions of Mg-9Al-0.6TiO_2, Mg-9Al-0.8TiO_2, Mg-9Al-1.0TiO_2 and Mg-9Al-1.2TiO_2 designated respectively as MA6T, MA8T, MA10T and MA12T. Since TiO_2 has not been directly added to magnesium alloy, the equivalent amount of TiO_2 added has been calculated on the basis of aluminum based composite added to magnesium for the synthesis of Mg-Al/Al_3Ti-Al_2O_3 composites. TiO_2 addition to magnesium based composite may be taken as indirect addition as estimated in the context of this work. The chemical composition of cast *in-situ* composites was analyzed by GBC AVANTA-M Atomic Absorption Spectrometers (AAS), Victoria, Australia.

The cast ingots of composite were sectioned vertically into two parts. One part was used for determining the properties of as-cast composites, while the other part was hot forged at 350 °C to reduce thickness by 30%. The microstructure of as cast and forged composites was examined under optical microscope, Olympus, PME3, Tokyo, Japan and field emission scanning electron microscope (FE-SEM), FEI QUANTA 200 FEG, Czech Republic. The picric acid-ethanol was used as etchant to reveal the grain structure and constituent phases. The porosity in a composite was estimated from the densities of the matrix alloy and the extracted oxide particles, determined by gravity bottle.

The Brinell hardness of the composites was measured at a load of 153.3 N with 2.5 mm diameter steel ball as indenter. The tensile tests of as cast and forged composites were carried out using cylindrical tensile specimens of gauge length 25 mm and diameter 5 mm, following ASTM–E8M specification, at a constant displacement rate of 0.2 mm/min using universal testing machine (Hounsfield S Series). Fractured surfaces of specimens after tensile tests were examined under scanning electron microscope (SEM).

Fracture toughness tests on C-T specimens of both as cast and forged composites were carried out following the standard ASTM E813-81 [18]. The specimen was pre-fatigued and load-load line displacement behaviour was measured with the help of clip-gage in order to arrive at J-R curve for the composites using single specimen. The crack length at different load was estimated from compliance by loading-unloading at different J-values. Initiation of the fracture toughness, J_{IC}, was determined for each material by the blunting line given by

$$J = 2M\sigma_f \Delta a \tag{1}$$

where $M = 1$ and $\sigma_f = \frac{1}{2}(\sigma_Y + \sigma_U)$. By shifting the blunting line through an offset distance of 0.2 mm away from *J*-axis, one arrives at the offset blunting line as prescribed by ASTM procedure. The intersection of this offset blunting line with the *J*-R curve gives the value of J_{IC} for the material.

The ductile crack propagation behaviour was characterized by the ratio of tearing modulus [19], *T*, to elastic modulus, *E*, as

$$T/E = \frac{1}{\sigma_f^2}\frac{dJ}{da} \tag{2}$$

where, d*J*/da is the slope of the *J* resistance curve and σ_f is flow stress of the material in the tension.

III. Results and Discussions

The Mg-Al/Al_3Ti-Al_2O_3 composites have been prepared, and Al-based composites have been developed in the first stage, by adding TiO_2 to molten Al-alloy. The TiO_2 particles are reduced by molten aluminum generating Al_2O_3 particles and releasing titanium to Al-alloy exceeding the solubility limit generating intermetallic compound of Al_3Ti. Thus, the resulting composite has both Al_3Ti and Al_2O_3 particles. This aluminum based composite has been added to the molten magnesium to maintain about 9 wt.% aluminum, and the after solidification, it will result in Mg-Al alloy based composite inheriting the constituents of the aluminum based composite developed earlier. The particle content in Mg-Al/Al_3Ti-Al_2O_3 composite has been varied by changing the amount of TiO_2 particles added to Al-alloy during the development of Al-alloy based composite in the first stage.

TABLE I
Chemical Compositions of as Received Commercial Mg and Al Ingots

Chemical composition (wt %)	Material	
	Mg-Ingot	Al-Ingot
Si	0.04	0.103
Fe	0.026	0.192
Zn	0.028	0.091
Cr	0	0.043
Ni	0.017	0.032
Mn	0.013	0.009
Cu	0.061	0.023
Al	0.031	99.479
Mg	99.784	0.028

The chemical composition of the cast composites MA6T, MA8T, MA10T and MA12T synthesized by addition of Al-06 wt.% TiO2, Al-08 wt.% TiO2, Al-10 wt.% TiO2 and Al-12 wt.% TiO2 alloys respectively and their intermetallic phases, Al3Ti, oxide particles contents are given in Table II. The density, the porosity and the grain size of these cast as well as forged composites and Mg-9 wt.% Al alloy designated as MA are given in Table III.

Figs. 1 (a) and (b) show respectively the typical microstructures of cast and forged magnesium based composites containing grayish rod like intermetallics, Al3Ti, inherited from aluminum based composite. The Al3Ti rods in cast composite, shown in Fig. 1 (a), break on hot forging into smaller lengths decreasing the aspect ratio considerably as observed in Fig. 1 (b).

The average aspect ratio of Al3Ti is about 7.5 in the cast structure but it decreases to 3 on forging. The β-phase, $Mg_{17}Al_{12}$ in Mg-Al phase diagram, which is relatively much smaller compared to Al_3Ti rods in cast composite appears as relatively bright particles, extended along the dendrite boundary in cast structure as shown in Fig. 1 (a). There are some dark spots which may be due to the shrinkage porosities or left behind by phases coming out during polishing. β-phase, $Mg_{17}Al_{12}$ appears to have decreased in the forged microstructure as evident in Fig. 1 (b) and it is attributed to elimination of segregation due to forging. β-phase dissolves during heating prior to forging and re-precipitate during cooling as finer particles than those observed in the cast microstructure. The grain size in the forged material is highly nonuniform, and there are relatively larger grains along with smaller grains at the boundary as shown in Fig. 1 (b). The rods of Al_3Ti have broken during forging, and there are cavities in between the broken segments as shown in Fig. 1 (b).

$Al_{12}Mg_{17}$ in the alloy gets partially dissolved and re-precipitates again on cooling as shown in Fig. 2 (b). The relatively larger grains in the microstructure of forged alloy as compared to that observed in the composite, as shown in Fig. 1 (b), is a clear indication that intermetallic, Al3Ti and oxides particles have acted as barrier to grain boundary movement during either dynamic recovery or recrystallization during hot forging. The smaller grains at the boundary of larger grains may be indicative of dynamic recrystallization in the grain boundary area, but the larger grains are possibly original deformed grains which may have undergone dynamic recovery.

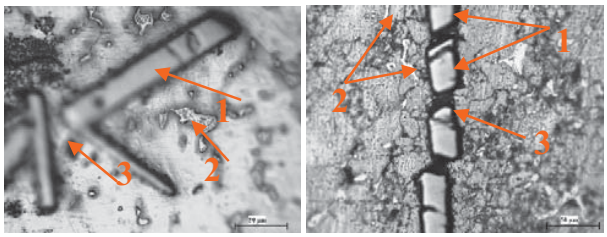

(a) MA10T-Cast (b) MA10T-Forged

Fig. 1 Typical optical Microstructures of cast and forged MA10T composites showing intermetallic Al_3Ti, β-phase, $Al_{12}Mg_{17}$, and oxide particles are marked 1, 2 and 3 respectively

To identify the different phases unambiguously, EDS has also been carried out on the forged sample to identify any change in phases or phase composition on the basis of chemical composition as shown in Fig. 3. There are relatively small bright particles along the grain boundaries marked 1 in SEM, which show more magnesium and less aluminum than β-$Al_{12}Mg_{17}$ observed in cast structure, which is possibly because of the signal from the exposed area below the particles. The number of small particles has increased in forged composites and it has been attributed to dissolution and re-precipitation β-$Al_{12}Mg_{17}$ during hot forging. The bright rod like Al_3Ti marked 2 has broken into several segments, as shown in Fig. 3 (b), during hot forging. The extended bright particles marked 3 in the SEM also belongs to β-$Al_{12}Mg_{17}$, as shown in Fig. 3 (c), and the presence of small titanium indicated could have been picked up from the matrix below the particle. The matrix marked 4 in the SEM, shows the presence of a small amount of titanium in the solid solution of aluminum in magnesium as shown in Fig. 3 (d). The chemical composition at the spot marked 5 in the SEM corresponds to Al_2O_3 as shown in Fig. 3 (e).

The optical micrographs of Mg-9 wt.% Al alloy as observed after casting and forging, are shown in Fig. 2. The microstructure shows the precipitates of intermetallic compound β-$Al_{12}Mg_{17}$ at the last freezing fraction of liquid at

dendrite boundaries. On hot forging, β-$Al_{12}Mg_{17}$ in the alloy gets partially dissolved and re-precipitates again on cooling as shown in Fig. 2 (b). The relatively larger grains in the microstructure of forged alloy as compared to that observed in the composite, as shown in Fig. 1 (b), is a clear indication that intermetallic, Al3Ti and oxides particles have acted as barrier to grain boundary movement during either dynamic recovery or recrystallization during hot forging. The smaller grains at the boundary of larger grains may be indicative of dynamic recrystallization in the grain boundary area but the larger grains are possibly original deformed grains which may have undergone dynamic recovery.

TABLE II
CHEMICAL COMPOSITIONS, Al_3Ti AND OXIDE CONTENTS IN CAST COMPOSITES

Designation	Target Composition	Reinforcements		Chemical composition (wt.%)		
		Intermetallic Al_3Ti (vol.%)	Extracted Oxide Particles (wt.%)	Al	Ti	Mg
MA6T	Mg-9Al-0.6TiO2	0.59 ± 0.25	1.22	9.48	0.21	Balance
MA8T	Mg-9Al-0.8TiO2	0.81 ± 0.22	1.51	9.23	0.26	Balance
MA10T	Mg-9Al-1.0TiO2	1.16 ± 0.28	1.85	9.14	0.31	Balance
MA12T	Mg-9Al-1.2TiO2	1.60 ± 0.32	2.56	9.15	0.35	Balance

TABLE III
DENSITY, POROSITY AND GRAIN SIZE IN Mg - Al ALLOY AND COMPOSITES

Designation	As-cast			Forged		
	Density	Porosity (vol.%)	Grain Size(μm)Matrix	Density	Porosity (vol.%)	Grain Size(μm)Matrix
MA	1.794	0.6	34	1.800	0.5	19
MA6T	1.799	0.7	33	1.812	0.6	18
MA8T	1.806	0.9	32	1.816	0.7	17
MA10T	1.816	1.4	31	1.829	1.0	16
MA12T	1.825	1.1	30	1.839	0.8	15

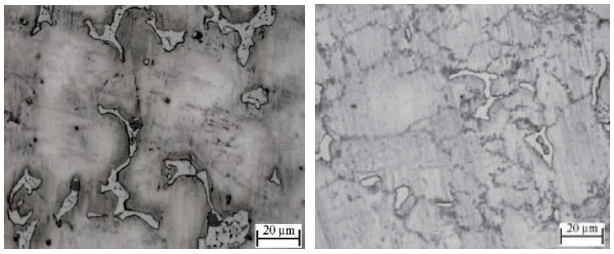

(a) (b)

Fig. 2 Optical micrographs of as cast and forged MA alloy; (a) MA-cast and (b) MA-forged

To identify the different phases unambiguously, EDS has also been carried out on the forged sample to identify any change in phases or phase composition on the basis of chemical composition as shown in Fig. 3. There are relatively small bright particles along grain boundaries marked 1 in SEM, which show more magnesium and less aluminum than β-$Al_{12}Mg_{17}$ observed in cast structure, which is possibly because of the signal from the exposed area below the particles. The number of small particles has increased in forged composites and it has been attributed to dissolution and re-precipitation β-$Al_{12}Mg_{17}$ during hot forging. The bright rod like Al_3Ti marked 2 has broken into several segments, as shown in Fig. 3 (b), during hot forging. The extended bright particles marked 3 in the SEM also belongs to β-$Al_{12}Mg_{17}$, as shown in Fig. 3 (c), and the presence of small titanium indicated could have been picked up from the matrix below the particle. The matrix marked 4 in the SEM, shows the presence of a small amount of titanium in the solid solution of aluminum in magnesium as shown in Fig. 3 (d). The chemical composition at the spot marked 5 in the SEM corresponds to Al_2O_3 as shown in Fig. 3 (e).

The variation of hardness averaged over the height of cast and forged ingots, with increasing wt.% of TiO_2 as shown in Fig. 4 (a) which also includes the corresponding properties of cast and forged MA alloy as a composite with zero wt.% of TiO2 content. There is significant improvement in hardness of both in the cast and the forged composites with increasing addition of TiO2 which are more or less similar if extrapolated to similar amount of reinforcement observed by Wang et al. [5], [6]. The average Brinell hardness of cast composite is higher by a factor about 1.2 than that observed in cast MA alloy. On hot forging, the hardness of the alloy and the composite increases over the corresponding cast material by about 100 and 80 BHN respectively as shown in Fig. 4 (a). The increase in hardness on forging may be attributed to the modification of microstructure taking place during forging as shown in Fig. 1 (b), apart from the decreasing porosity on forging as shown in Table III.

The variations in room temperature tensile properties – yield strength, UTS and percentage elongation of cast and forged Mg-Al/Al_3Ti-Al_2O_3 composites with increasing wt.% of TiO_2 designated as MA6T, MA8T, MA10T and MA12T as well as MA alloy (indicated by zero reinforcement) are shown in Figs. 4 (b)-(d), respectively. In cast composites, the yield strength decreases from 123.5 MPa in MA alloy progressively till 98 MPa in the composite synthesized by addition of about 1.0 wt.% of TiO2, but beyond this level of TiO2 addition, the yield strength increases and the porosity as indicated in bracket, decreases, similar to that observed by Lu et al [8] for the mechanically alloyed composite. In forged composites, yield strength increases with increasing TiO_2 addition of about 0.8 wt.% TiO_2, but it decreases with increasing TiO_2 till

addition of about 1.0 wt.% of TiO_2 but further increase in TiO_2 addition increases the yield strength as shown in Fig. 4 (b). The UTS for cast and forged composites as shown in Fig. 4 (c), follows the same trend of variation as the yield strength but the extent of variation is more than that observed in case of yield strength. Porosity [20], [21] increases in cast composites with increase in TiO_2 addition, as given in Table III and the effect of increasing TiO_2 addition is more than balanced by the counter-effect of increasing porosity. The yield strength and UTS of forged composites are higher and the porosity is lower than their cast counterpart. The ductility of the forged composites is lower than those observed in cast composites as shown in Fig. 4 (d), in spite of lower porosity. The ductility decreases with increasing wt.% of TiO_2 addition in both cast and forged composites till addition of 1.0 wt.% of TiO_2 but beyond this level of TiO_2, the ductility increases and porosity decreases slightly. The increase in strength may be attributed to the refined microstructure and some healing of pores.

In forging, the particle clustering, which increases at higher particle content, and the degree of deformation strain have been found to be important in determining the strength. At higher strain, the clustered particles often move apart but the matrix alloy is prevented by the particles around from flowing in to fill the gap. Under these circumstances, porosity increases on forging and strength deteriorates [22]. In the present experiment, the porosity has not increased on forging and so, the lower strength at higher TiO_2 addition, may be attributed to extensive cracking of Al_3Ti particles as shown in Fig. 1 (b).

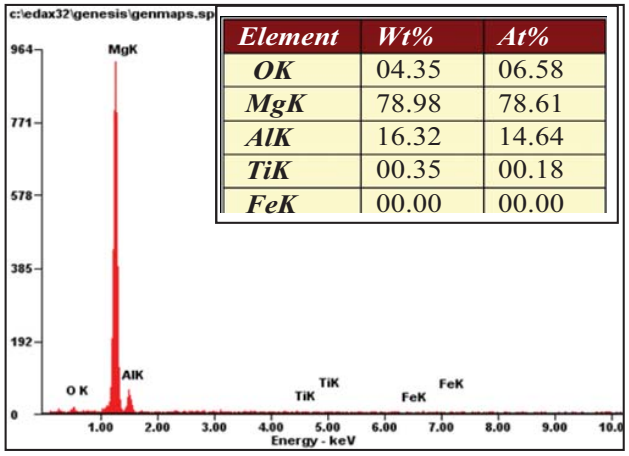

Element	Wt%	At%
OK	04.35	06.58
MgK	78.98	78.61
AlK	16.32	14.64
TiK	00.35	00.18
FeK	00.00	00.00

(a)

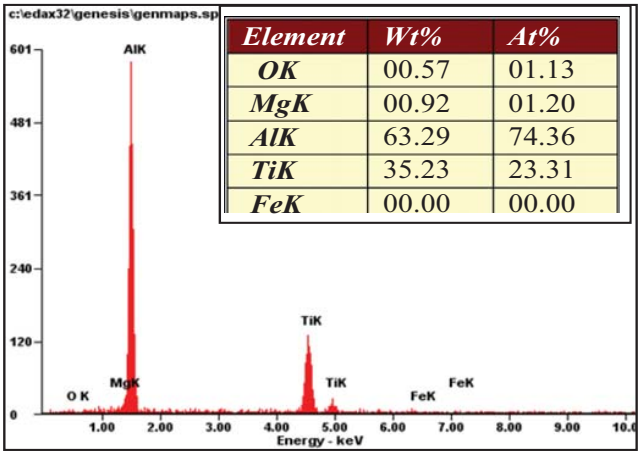

Element	Wt%	At%
OK	00.57	01.13
MgK	00.92	01.20
AlK	63.29	74.36
TiK	35.23	23.31
FeK	00.00	00.00

(b)

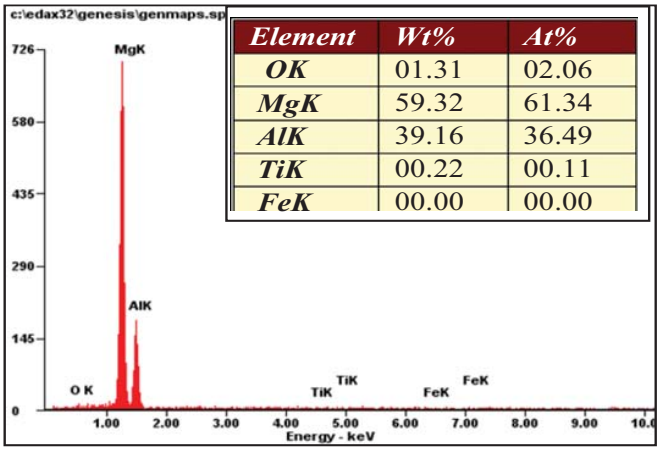

Element	Wt%	At%
OK	01.31	02.06
MgK	59.32	61.34
AlK	39.16	36.49
TiK	00.22	00.11
FeK	00.00	00.00

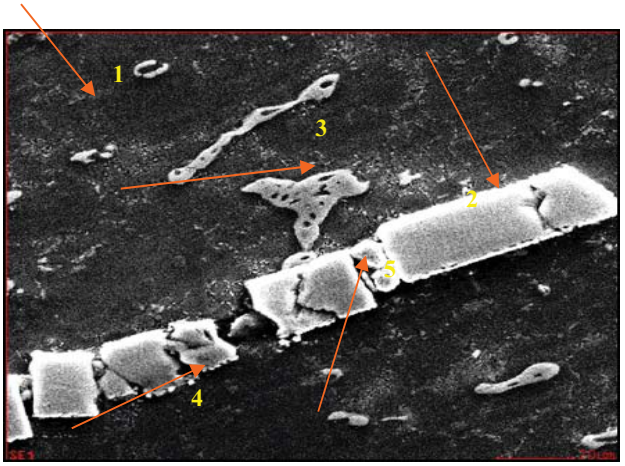

(c)

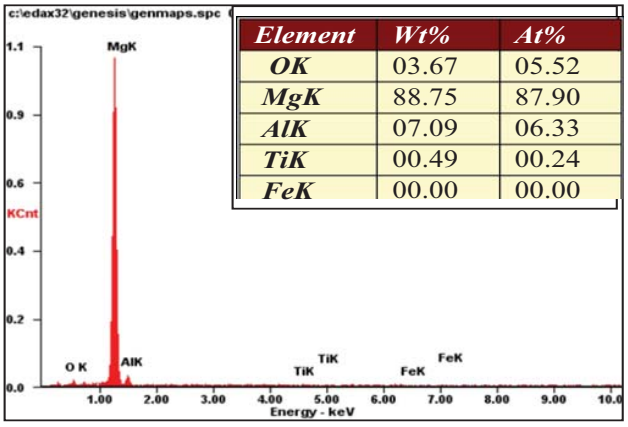

Element	Wt%	At%
OK	03.67	05.52
MgK	88.75	87.90
AlK	07.09	06.33
TiK	00.49	00.24
FeK	00.00	00.00

(d)

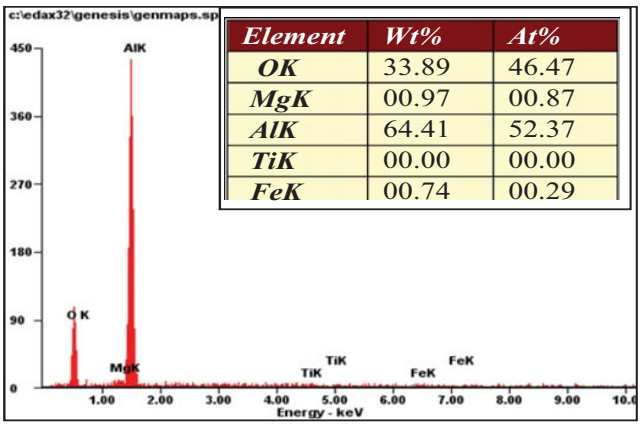

Element	Wt%	At%
OK	33.89	46.47
MgK	00.97	00.87
AlK	64.41	52.37
TiK	00.00	00.00
FeK	00.74	00.29

(e)

Fig. 3 EDS point analysis of the matrix and different types of particles in forged Mg-Al/Al_3Ti-Al_2O_3 composite designated MA8T

The ductility decreases with increasing wt.% of TiO_2 addition in both cast and forged composites but forging has reduced the ductility not only in the composite but also in the alloy, as shown in Fig. 4 (d). The ductility of the alloy should have improved because of removal of segregation, some porosity and refined microstructure but it has not happened, possibly due to remaining strain in the forged alloy which may be reflected in its increased hardness as shown in Fig. 4 (a). It is also possible that there is micro-cracking of Mg/$Mg_{17}Al_{12}$ interface and even in the $Mg_{17}Al_{12}$ particles as observed by Lu et al. [4]. In the composites, remaining matrix strain has been compounded by particle fracture and so, the ductility decreases with increasing wt.% of TiO_2 addition. However, the ductility in the cast and forged composites are similar to those observed in AZ91 alloy based composites [7].

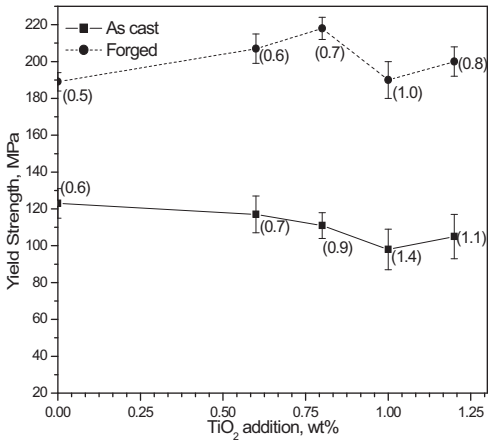

(b)

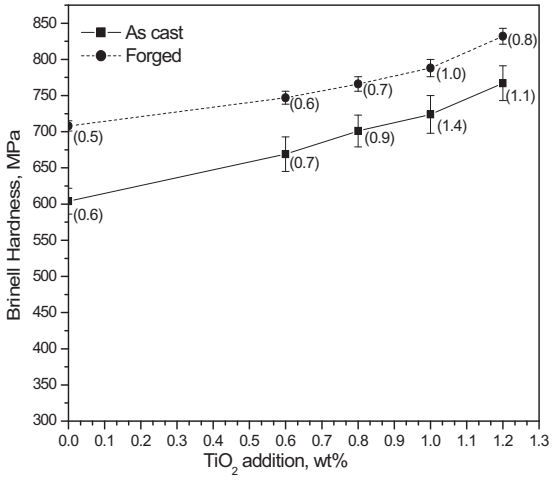

(a)

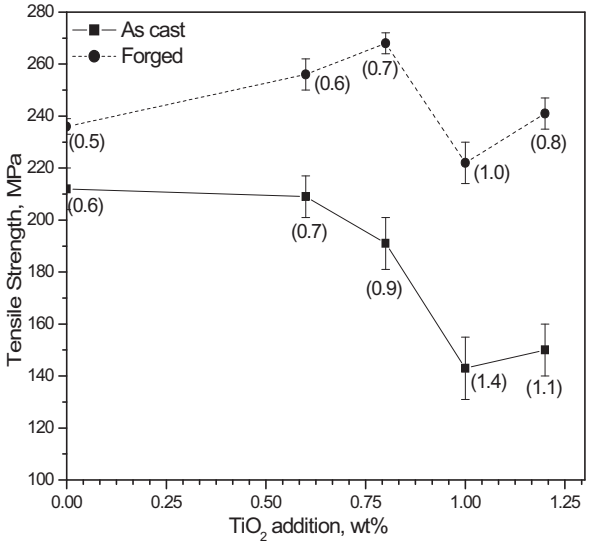

(c)

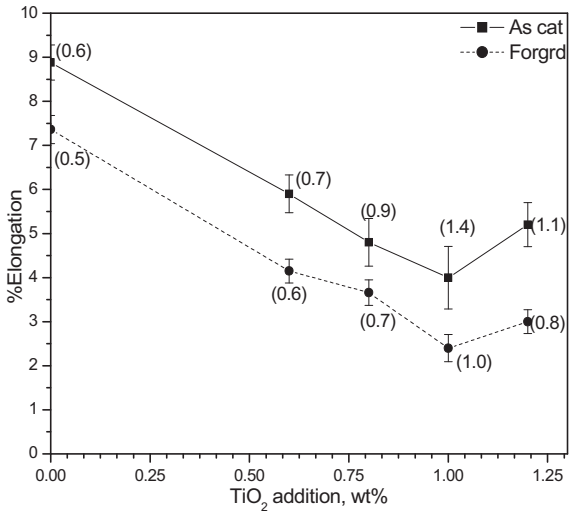

(d)

Fig. 4 Variation of mechanical Properties in cast and forged composite with increasing wt.% of TiO_2 addition: (a) Hardness, (b) Yield strength, (c) Tensile strength and (d) Percentage elongation

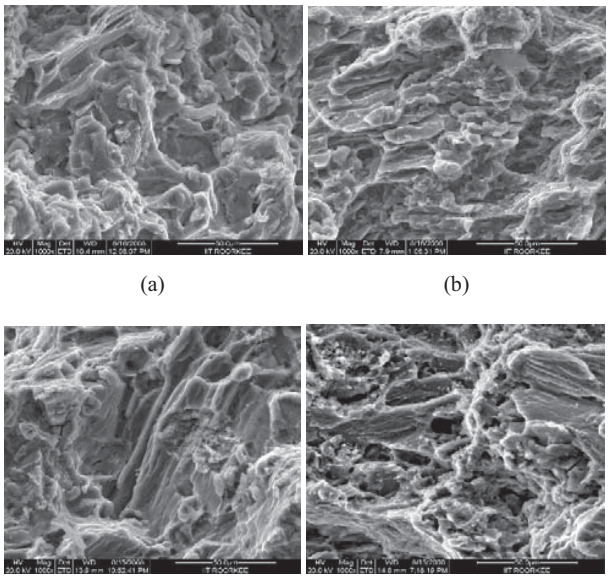

(a) (b)

(c) (d)

Fig. 5 SEM fractographs showing tensile fracture surfaces of (a) cast MA6T, (b) forged MA6T, (c) cast MA12T and (d) forged MA12T

The fractured surfaces of tensile specimens of cast and forged composites are shown in Fig. 5. The fractured surfaces of cast composites of MA6T and MA12T shown in Figs. 5 (a) and (c) reveals the evidence of debonding of alumina particles and growth of voids leading to dimples, which are relatively shallow because of limited ductility of the composites. There are also cleaved regions, which may have taken place along the interface of the matrix with Al_3Ti rods. The fractured surfaces of forged composites of MA6T and MA12T are shown in Figs. 5 (b) and (d) respectively. The debonded and cleaved surface features are slightly smaller compared to those observed in their cast counterparts and it may be the consequence of finer microstructure and fractured Al_3Ti as observed after forging.

The *J-R* curves of cast alloy and composites containing different intermetallic, Al_3Ti, and oxide contents are shown in Fig. 6 (a), and the lines drawn are regression fit of the experimental points representing ductile crack propagation. The *J-R* curves for the forged alloy and composites are given in Fig. 6 (b). There is a drastic increasing of *J-R* curve from that for cast alloy to those of cast composites but the *J-R* curves for forged alloy and composites are relatively low as compare to cast counterparts. Initiation fracture toughness, J_{IC}, for both cast and forged alloy and composites have been obtained by drawing offset blunting line for each material as outlined in the experimental procedure. For the cast alloy, the observed J_{IC} is 10.2 X 10^{-3} MPa m, which is higher than that observed by Barbagallo et al. [17] in sand cast AZ91C subjected to T6 heat treatment. The J_{IC} increases from cast MA alloy to cast composites due to the presence Al_3Ti and oxides particles as shown in Fig. 8. But, Purazrang et al. [15] have observed the decrease of K_{IC} when AZ91 alloy is reinforced by short alumina fibers. There is drastic reduction of J_{IC} on forging of MA alloy and it could be attributed to lowering of ductility on forging. The J_{IC} for the forged alloy and the composites are relatively lower than the cast counterparts. The boundary of fine grains with precipitate at the boundary of large grains as shown in Fig. 2 (b) may have provided low energy path for ductile crack propagation. In the forged composites, the weakness of the forged matrix alloy has been further compounded by breaking of Al_3Ti rods in addition to incomplete recovery of forging strain. The voids between the broken segments of Al_3Ti rods are shown in Fig. 1 (b). All these factors decrease J_{IC} by about 50 pct. compared to their cast counterpart.

The ratio of tearing modulus to elastic modulus (*T/E*) has been determined by dividing the slope of the *J-R* curve with the square of flow stress as expressed in (2), and this ratio indicates the resistance to ductile crack propagation. In comparison to the cast alloy, the composites show lower ratio, but with increasing intermetallic, Al_3Ti, and oxide contents, the ratio increases and then decreases as shown in Fig. 7.

The presence of intermetallic, Al_3Ti, and oxide particles is detrimental for *T/E* ratio, which is prone to cracking as it has been observed after forging. After forging, the *T/E* ratio of the alloy decreases comparatively more than those in cast composites and it is indicative of damage caused by the change in the microstructure and the loss in ductility on forging of the alloy. In forged composite, presence of both intermetallics, Al_3Ti, oxide contents and the forged matrix microstructure decreases the ratio significantly but it becomes insensitive to increasing intermetallic, Al_3Ti, and oxide contents as sufficient damage has already been done from the standpoint of *T/E* ratio.

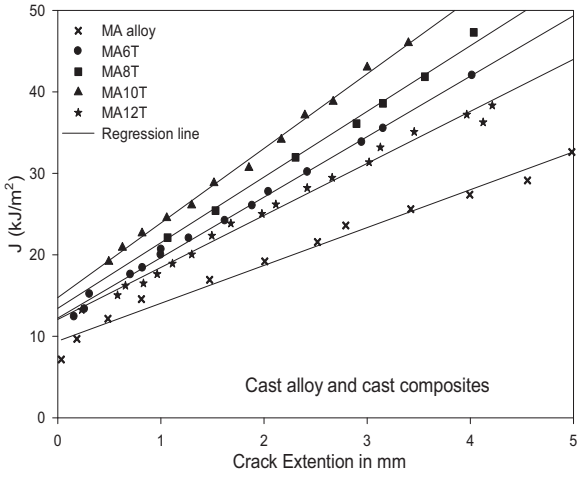

(a)

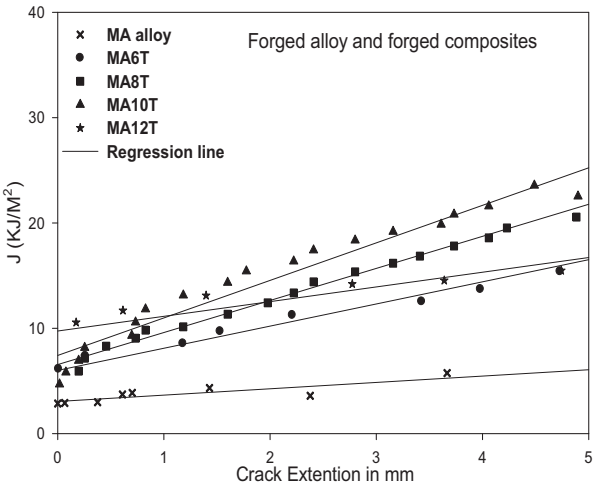

(b)

Fig. 6 J-R curves of: (a) cast alloy and cast composites and (b) forged alloy and forged composites

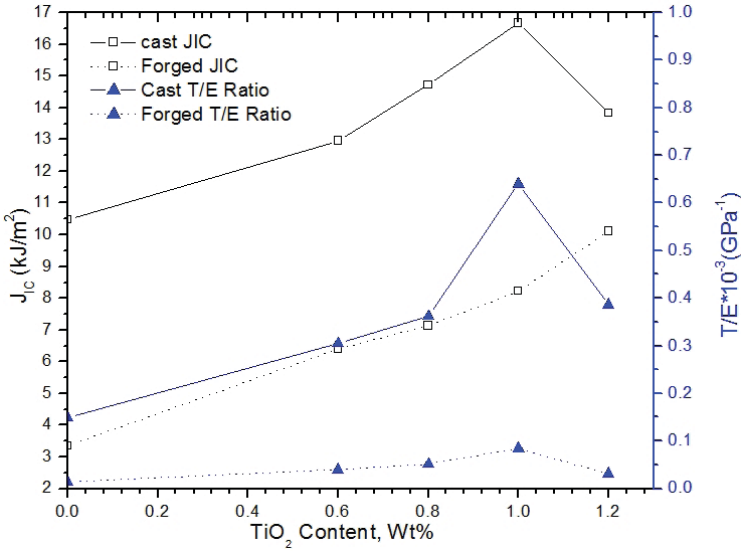

Fig. 7 Variation of initiation fracture toughness, J_{IC}, ratio of tearing modulus to elastic modulus of cast and forged composites with different wt.% of TiO_2

IV. Conclusion

In Mg-Al/Al_3Ti-Al_2O_3 composite, Al-based composites have been developed in the first stage, by adding TiO_2 to molten Al-alloy, resulting composite has both Al_3Ti and Al_2O_3 particles. This aluminum based composite has been added to molten magnesium result in Mg-Al alloy based composite inheriting the constituents of the aluminum based composite developed earlier. The particle content in Mg-Al/Al_3Ti-Al_2O_3 composite has been varied by changing the amount of TiO_2 particles added to Al-alloy during the development of Al-alloy based composite in the first stage. The mechanical properties of cast and forged composites were investigated and compared with those observed in cast and forged commercial magnesium and Mg-9 wt. pct. alloy processed similarly as the composites. The present study has led to the following conclusion.

1. The cast microstructure of Mg-Al/Al_3Ti-Al_2O_3 composites show dendrites of α-Mg and β-$Al_{12}Mg_{17}$ in the inter-dendritic region, as it has been observed in MA alloy.
2. Intermetallic of Al_3Ti is distributed in the matrix of Mg-Al/Al_3Ti-Al_2O_3 composites apart from oxide inclusions formed during processing. Also Al_2O_3 particles formed by reaction of TiO_2 with aluminum in aluminum based composite, which has been added to molten magnesium to prepare this composite.
3. Forging refines β-$Al_{12}Mg_{17}$ in the matrix and removes dendritic segregation. Some of Al_3Ti rods inherited from

aluminum based composites are attacked by magnesium on the surface and in a few rods even segments of rods have been reduced to particles.

4. There is dynamic recrystallization stimulated by presence of particles in the grain boundary region. However, the body of large grains has shown dynamic recovery.
5. Forging results in extensive cracking of the intermetallic Al_3Ti and also, creates voids inside the particle clusters.
6. The Brinell hardness of cast composites increases with increasing particle content. In forging of composites has resulted in similar increase in hardness as observed in the matrix alloy and so, the increase might be attributed to incomplete recovery of forging strain in the matrix of the composite.
7. The yield strength in cast composite decreases with increasing particle content, it may be attributed to dominating contribution of increasing casting defects with increasing particle content in cast Mg-Al/Al_3Ti-Al_2O_3 composites.
8. On forging, the yield strength increases in the composites with increasing particle content as forging heals the defects of segregation and porosity to an extent and restores the trend expected.
9. In cast composites, UTS decreases with increasing particle content. It may be attributed to progressive debonding of particles during plastic deformation. But after forging, UTS is observed to increase at relatively lower particle content as the ductility decreases after forging but thereafter, increased clustering of particles and creation of more voids during forging lowers the observed UTS.
10. On forging, the ductility decreases due to incomplete recovery of forging strain in the composites and so, the extent of debonding decreases during plastic deformation in forged composites.
11. In cast composites, J_{IC} increases with increasing particle content. Because of small particles of oxide and Al_3Ti rods in cast Mg-Al/Al_3Ti-Al_2O_3 composites may be blunting cracks. But after forging, J_{IC} decreases compared to their cast counterpart in the composites, which is attributed to the increased brittleness compounded by cracking of Al_3Ti particles, but the trend of variation observed in cast composites with increasing particle content still remains after forging.
12. Resistance to crack propagation is adversely affected not only by alloying, incorporation of particles and increased clustering at higher particle content but also by the loss of ductility and cracking of particles after forging.

REFERENCES

[1] Y.C. Lee, A.K. Dahle, D.H. St John: Metall. Trans A, 2000, vol. 31A, pp. 2895.
[2] I.J. Polmear: Mater. Sci. Technol., 1994, vol. 10, pp. 1.
[3] Z. Zhang, A. Couture, A. Luo: *Scrip. Metall.*, 1998, vol. 39, pp. 45.
[4] Y.Z. Lu, Q.D. Wang, W.J. Ding, X.Q. Zeng, Y.P.Zhu: Mater. Let., 2000, vol. 44, pp. 265-8.
[5] H.Y. Wang, Q.C. Jiang, Y .Wang, B.X. Ma, F .Zhao: Mater. Let., 2004, vol. 58, pp. 3509-13.
[6] Wang Yan, Wang Hui-Yuan, Xiu Kun, Wang Hong-Ying, Jiang Qi-Chuan: Mater. Let., 2006, vol.60, pp. 1533-7.
[7] D.J. Lloyd: Int. Mater. Rev., 1994, vol. 39, pp. 1-23.
[8] Hassan, S.F., Gupta, M.,: *J. of Alloys and Compounds*., 2002, vol. 345, pp. 246-251.
[9] N. Ogawa, M. Shiomi, K. Osakada: Mach. Too. Manuf., 2002, vol. 42, pp. 607-14.
[10] B.N. Behrens, I. Schmidt: Mater. Proc. Technol., 2007, vol. 187-188, pp. 761-765.
[11] Hong Tae Kang, Terry Ostram: Mater. Sci. Eng., 2008, vol. 490, pp. 52-6.
[12] V. Laurent, Jarry, G. Regazzoni: J. Mater. Sci., 1992, vol. 27, pp. 4447-59.
[13] H. Somekawa, T. Mukai: Scripta Mater., 2005, vol. 53, pp. 1059-1064
[14] K. Purazrang, K. U. Kainer, B. L. Mordike: Composite, 1991, vol. 22, pp. 456–462.
[15] K. Purazrang, P. Abachi, K. U. Kainer: Composite, 1994, vol. 25, pp. 296–302.
[16] M. Manoharan, J. Lewandowski: J. Acta metall. Mater, 1990, vol.38, No. 3, pp.489-196.
[17] S. Barbagallo, E. Cerri: Eng. Fail. Anal., 2004: vol. 11, pp.127-40.
[18] ASTM Annual Book of Standards: Am. Soc. Test. Mater., 1987, E-813, pp. 713.
[19] P.C. Paris, H. Tada, A. Zahoor and E. Ernst: ASTM STP 668, Am. Soc. Test. Mater, 1979, pp. 5.
[20] H.L. Rizkalla, A, Abdulwahed: J. Mater. Proc. Technol., 1996, vol. 56, pp. 398– 403.
[21] S.M.L. Nai, M. Gupta: Compos. Struct., 2002, vol. 57, pp. 227–33.
[22] L.Ceschini, G Minak, and A. Morri, Comp. Sci. Technol., 2009, vol. 69, pp. 1783-89

Dr. H. M. Nanjundaswamy, B.E., M.Tech. PhD (IITR), MIE. MISTE, e-mail: hmnanjunda@gmail.com, Cell: +91-9481830134, Ph: +91-08232-220043-246, Fax: +91-08232-222075, Res: +91-9481150262

Dr. H. M. Nanjundaswamy, born in Harohally, a village in Karnataka of the Indian subcontinent on 10th May 1972. He is Bachelor of Engineering from the University of Mysore, Mysore, Karnataka, India (1994), Master of Technology in Production Engineering, from the University of Mysore, Mysore and Doctorate from Indian Institute of Technology, Roorkee, Roorkee, Utherkhand, India (2010). His major field of study is Composites, Fracture Toughness.

He is Professor and Head of the Department of Industrial and Production Engg., at PES College of Engineering, Mandya Karnataka, India (PIN-571401) which is affiliated to Visvesvaraya Technological University, Belagavi.

He has published many papers on Synthesis and characterization of composites (MMC) and secondary processes like forging extrusion of aluminum and magnesium composites. His research interests are composites MMC, PMC and Nano-composites.

The author is a Member of Institution Engineers (India) (2010) and Member of Indian Society for Technical Education (2001).